Star Formation Newsletter #336 1-8

Yusuke Aso (KASI)

Resolving the outer ring of HD 38206 using ALMA and constraining limits on planets in the system

Mark Booth [1]★ Michael Schulz,[1] Alexander V. Krivov,[1] Sebastián Marino [2,3] Tim D. Pearce [1] and Ralf Launhardt[2]

- デブリ円盤から惑星の場所を制限できる。
- HD38206: Herschel（θ ~6"）からi=60°に近く、11 auと160 au（幅11 au）にベルト。Columba association (71 pc, 42 Myr、若い)。
- ALMA Cy 1, 213, 215, and 228 GHz, 0.97"x0.75"。160 μmと合わせてダストβ=0.6。CO 2-1は検出無し。

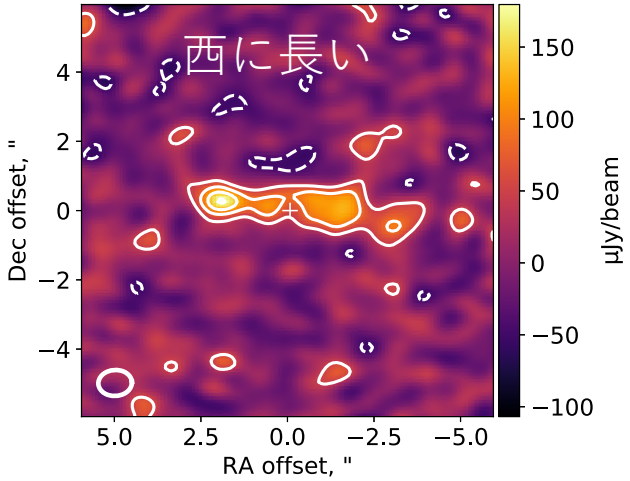

- ガウシアン3D離心リングモデル。
- パラメーターはa0, Δa, M_{dust}, i, PA, e, ω。

$$a(r,\phi) = r\frac{1-e\cos(\phi-\omega)}{1-e^2},$$

$$\Sigma(r,\phi,z) \propto \exp\left(-\frac{(a-a_0)^2}{2\sigma_r^2} - \frac{z^2}{2h^2r^2}\right),$$

- Spwごとのビジビリティをスペクトル指数2.6としてフィット。
- null modelでχ^2=2N_{vis}となるように重みをスケール。RADMC3D, EMCEE。
- Herschelより幅広でエッジオン。

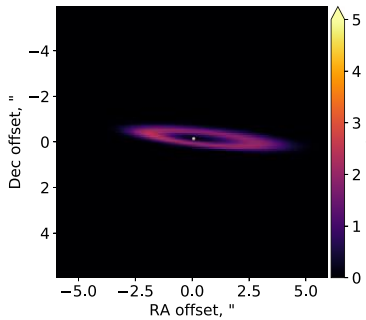

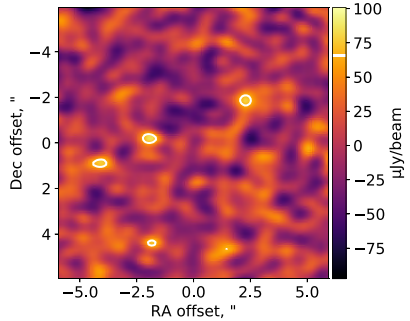

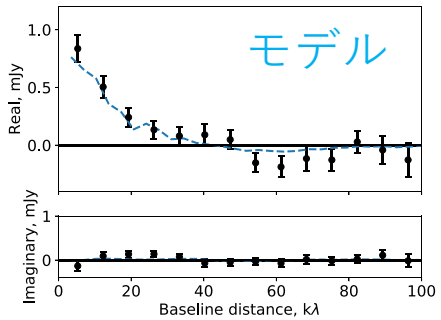

a_0 (au)	Δa (au)	M_{dust} ($M_\oplus$)	I (°)	Ω (°)	e	ω (°)
184^{+19}_{-17}	143^{+46}_{-36}	$0.105^{+0.016}_{-0.015}$	$83.3^{+1.3}_{-1.3}$	$84.3^{+1.2}_{-1.2}$	$0.25^{+0.10}_{-0.09}$	49^{+22}_{-25}

Resolving the outer ring of HD 38206 using ALMA and constraining limits on planets in the system

の続き

Mark Booth [1]★ Michael Schulz,[1] Alexander V. Krivov,[1] Sebastián Marino [2,3] Tim D. Pearce [1] and Ralf Launhardt[2]

次がわかっている。惑星は必要か？
(i)カスケードでダストができるほど微惑星が撹拌。
(ii)内側と外側のリングのギャップ。
(iii)非対称は動的相互作用。

$$T_{\rm s} = 9.3\,{\rm Myr}\left(\frac{1}{\gamma}\right)\left(\frac{\rho}{1\,{\rm g\,cm^{-3}}}\right)^{-1}\left(\frac{v_{\rm frag}}{30\,{\rm m\,s^{-1}}}\right)^{4}\left(\frac{S_{\rm max}}{200\,{\rm km}}\right)^{-3} \times \left(\frac{M_\star}{{\rm M}_\odot}\right)^{-1/2}\left(\frac{a_0}{100\,{\rm au}}\right)^{7/2}\left(\frac{\Delta a/a_0}{0.1}\right)\left(\frac{M_{\rm disc}}{100\,{\rm M}_\oplus}\right)^{-1}$$

- 200 kmの微惑星がいくつかあったなら13 Myrで十分撹拌（Krivov&Booth18）。
- 小惑星帯とカイパーベルトのようにギャップは惑星を示唆。
- 同じ平面、同じ質量、円、log uniform spacingのとき必要な個数。
  ギリギリ安定な最大個数。その2倍の間隔でもギリギリ掃ける（最小個数）。

$$N_p = \frac{\log_{10}(a_{\rm in}/a_{\rm w})}{\log_{10}(1+g\delta_{\rm min})}$$

$$\delta_{\rm min} = \frac{\mu^{1/4}}{3.7}(\log_{10}(\tau/{\rm yr}) + 1 + \log_{10}(\mu/10^{-7})),$$

- 20 or 16ヒル半径離れた惑星が42 Myr以内に間の微惑星を散らす。

$$m_{\rm p} = \left(\frac{\kappa}{\tau}\right)\left(\frac{a_{\rm in}}{1\,{\rm au}}\right)^{3/2}\left(\frac{M_\star}{{\rm M}_\odot}\right)^{1/2} m_\oplus\,,$$

$$N_{\rm p} = 1 + \frac{\log_{10}\left(\frac{a_{\rm in}}{a_{\rm w}}\right)}{\log_{10}\left(\frac{1+0.006K\left(\frac{m_{\rm p}}{{\rm M}_\oplus}\right)^{1/3}\left(\frac{M_\star}{{\rm M}_\odot}\right)^{-1/3}}{1-0.006K\left(\frac{m_{\rm p}}{{\rm M}_\oplus}\right)^{1/3}\left(\frac{M_\star}{{\rm M}_\odot}\right)^{-1/3}}\right)},$$

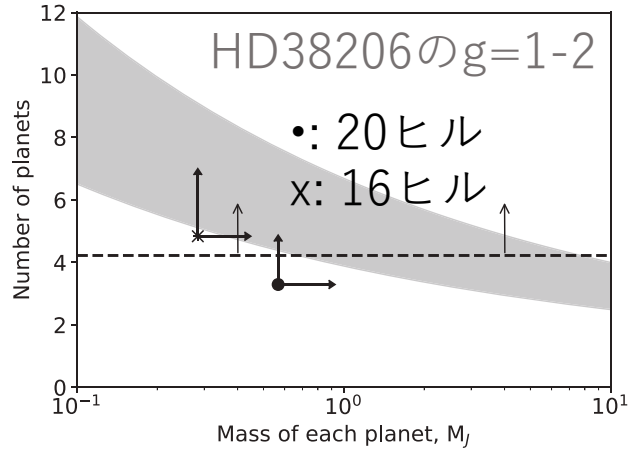

- 外の惑星が永年摂動で円盤を直接撹拌。
  $e_{\rm p} = 0.34^{+0.20}_{-0.13}$, $m_{\rm p} = 0.7^{+0.5}_{-0.3}\,{\rm M_J}$ and $a_{\rm p} = 76^{+12}_{-13}$ au. 質量感度10倍で見える。

$$t_p \approx 1.53\times10^3\frac{\left(1-e_{\rm p}^2\right)^{3/2}}{e_{\rm p}}\left(\frac{a_{\rm out}}{10\,{\rm au}}\right)^{9/2} \times\left(\frac{M_\star}{{\rm M}_\odot}\right)^{1/2}\left(\frac{m_{\rm p}}{{\rm M}_\odot}\right)^{-1}\left(\frac{a_{\rm p}}{1\,{\rm au}}\right)^{-3}{\rm yr},$$

$$m_{\rm p} = \frac{1}{125}\left(\frac{a_{\rm in}}{a_{\rm p}(1+e_{\rm p})}-1\right)^3(3-e_{\rm p})M_\star.$$

$$e_{\rm p} = \frac{4}{5}\frac{a}{a_{\rm p}}e.$$

Dynamical stellar masses of pre-main sequence stars in Lupus and Taurus obtained with ALMA surveys in comparison with stellar evolutionary models

Teresa A. M. Braun,[1] Hsi-Wei Yen,[1] Patrick M. Koch,[1] Carlo F. Manara,[2] Anna Miotello,[2] and Leonardo Testi[2,3]

- 正確なIMFのためにM_{spec}（PMSでばらつく）をM_{dyn}で校正。
- ALMA, 0.12"-0.25", 1-3 Myr, Lupus & Taurus (~150 pc)。
- ダスト円盤からi, PAを決められるもの30 (Lupus) + 37 (Taurus)。
- 輝線の感度が不十分でも^{13}CO, C^{18}O J=2-1, 3-2（あればCNも）をスタック。
- 薄いケプラー円盤を基準としたラインプロファイルをスタックして最高のS/NになるM_*とv_{sys}。
- プロファイルをガウシアンフィットしてガウシアンの重みで±1σを積分して信号とする。
- ピーク<4σや線幅<3 chansは不採用。空間は95%フラックス半径。エラーバーはχ^2で50%まで。
- 3DモデルDALIでチェック。i>70°ではM_*を30%過大評価。

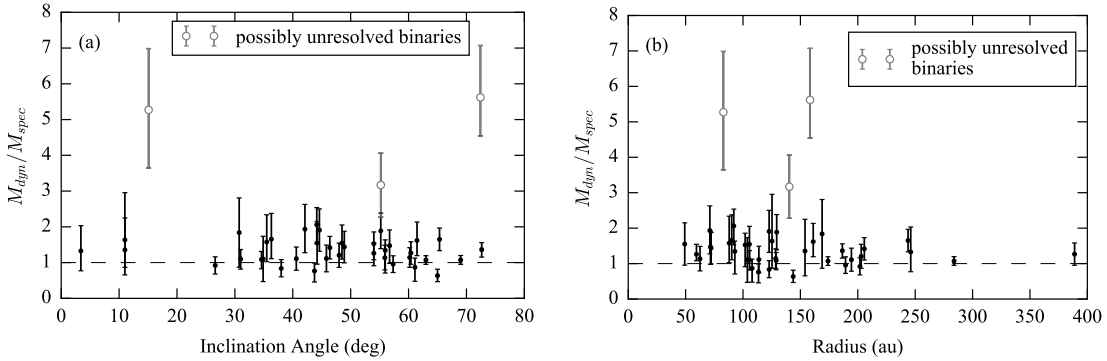

M_*とi, R, M_{gas}, Σ に相関はないのでバイアス無し。

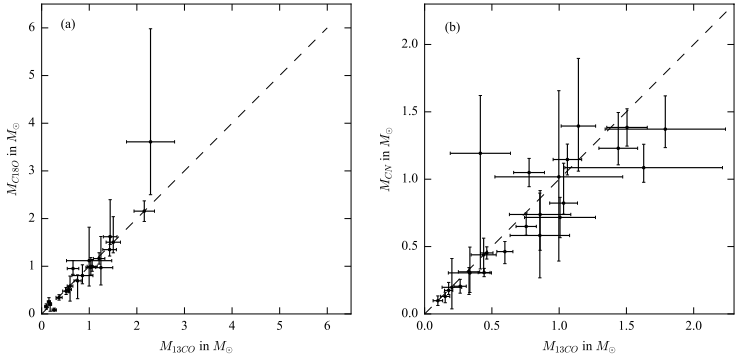

分子種による差も無し。

- 高感度観測とも合う（Dとiをスケール後）。
- T_{eff}を５つに分けてM_{dyn}が中央値より3倍外れるものは連星候補。

Dynamical stellar masses of pre-main sequence stars in Lupus and Taurus obtained with ALMA surveys in comparison with stellar evolutionary models

Teresa A. M. Braun,[1] Hsi-Wei Yen,[1] Patrick M. Koch,[1] Carlo F. Manara,[2] Anna Miotello,[2] and Leonardo Testi[2,3]

の続き

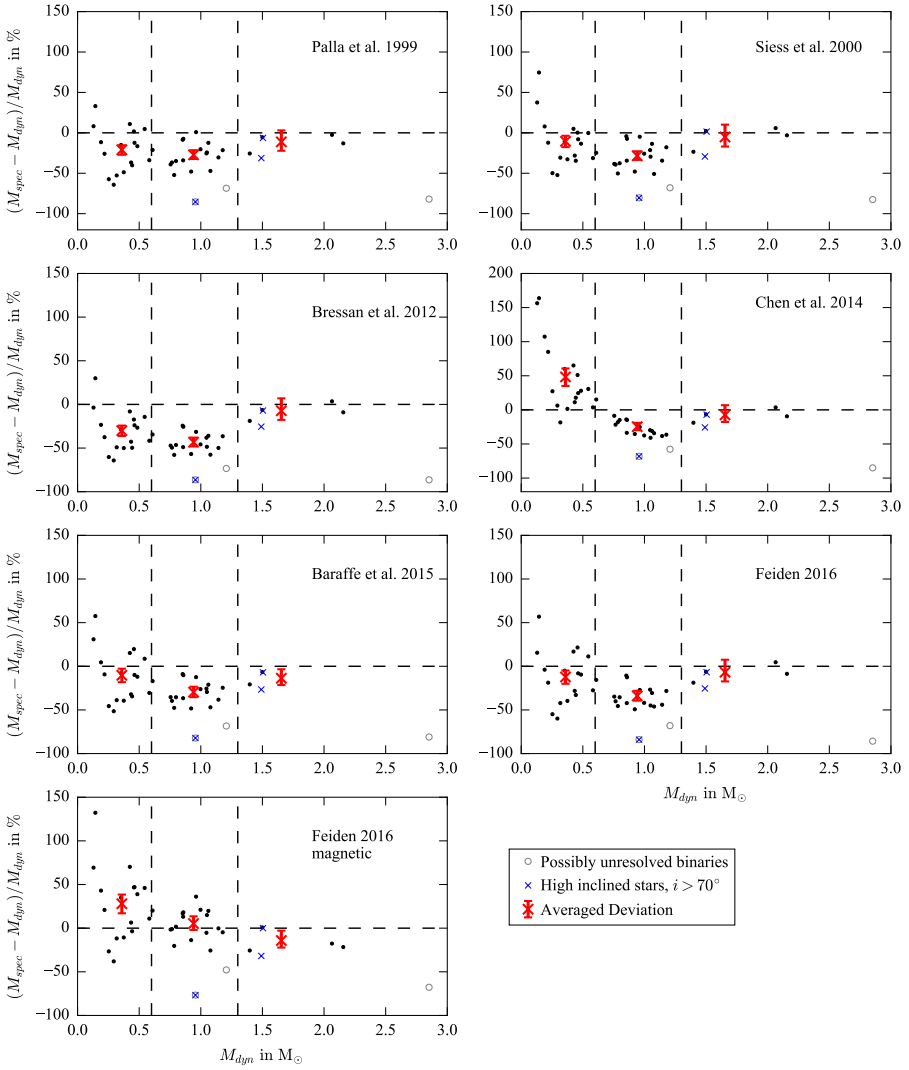

- M_*<0.6 M_{sun}ではBHAC15, F16, SFD00が1.6 σで合う。
- 0.6 – 1.3 M_{sun}はmagnetic F16のみ合う。他は20-40%過小評価。
- magnetic F16が正しい場合、磁場でゆっくり収縮するのでT Tauri期が長い可能性。
- しかし、magnetic F16は<0.6 M_{sun}を説明できないので、星進化の物理がM_*に依ることを示唆。

C14, BHAC15, F16: non-gray boundary、オパシティが周波数で違う。
PS99, Br12: gray boundary。
SFD00: non-grayの解析的フィット。
✓ 対流のmixing lengthもそれぞれ違う。
✓ magnetic F16以外non-magnetic。

H_2 mass–velocity relationship from 3D numerical simulations of jet-driven molecular outflows

A. H. Cerqueira[1], B. Lefloch[2], A. Esquivel[3], P. R. Rivera-Ortiz[2], C. Codella[4,2], C. Ceccarelli[2], and L. Podio[4]

- ジェット/ウインドが分子流を作るシナリオは$m(v) \propto v^{-\gamma}$ or $\exp(-v/v_0)$を説明できるか。
- collimated jetとambientの相互作用が有力。化学流体シミュレーションYguazu-aで混ざり具合も調べる。
- 2, 2, 8x104 au, 256x256x1024、5層、 Δx=78.13 au。半径5Δxのジェット。

Model	$v_{j,0}$ (km s^{-1})	A	n_a (cm^{-3})	n_j (cm^{-3})	η	T_a (K)	T_j (K)	τ_P (yr)	θ (°)	N_{tot}	τ_e (yr)
DR_SS	212	0	100	100	1	100	1000	–	–	–	–
DR	212	0.15	100	100	1	100	1000	–	–	4	5, 10, 20 and 50
DR_P	212	0.15	100	100	1	100	1000	200	6	4	5, 10, 20 and 50

歳差や正弦パルス。

$$H + H_2 \rightarrow 3H,$$

$$H_2 + H_2 \rightarrow 2H + H_2,$$

$$e + H_2 \rightarrow e + 2H.$$

分子は原子の9倍
イオンは原子の1%

- 視線x方向からi傾ける。 Δv=1 km/sで$m(v)$を計算。
- 初めにjetとambientをj=0, 1で区別して、混ざり具合を見る。 $j<j_{mix}$を取り出せる。

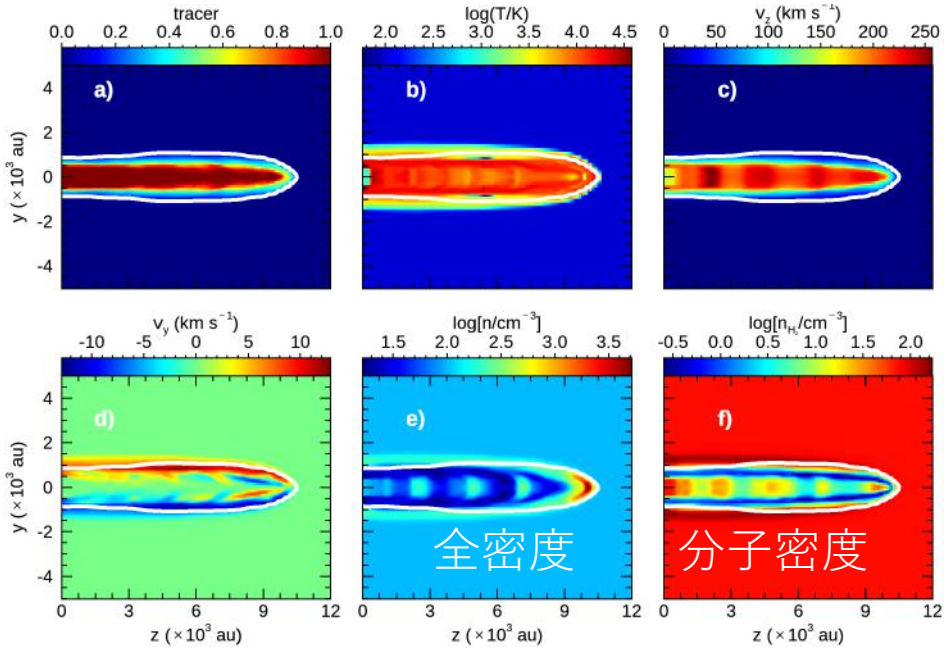

H_2 mass–velocity relationship from 3D numerical simulations of jet-driven molecular outflows

A. H. Cerqueira[1], B. Lefloch[2], A. Esquivel[3], P. R. Rivera-Ortiz[2], C. Codella[4,2], C. Ceccarelli[2], and L. Podio[4]

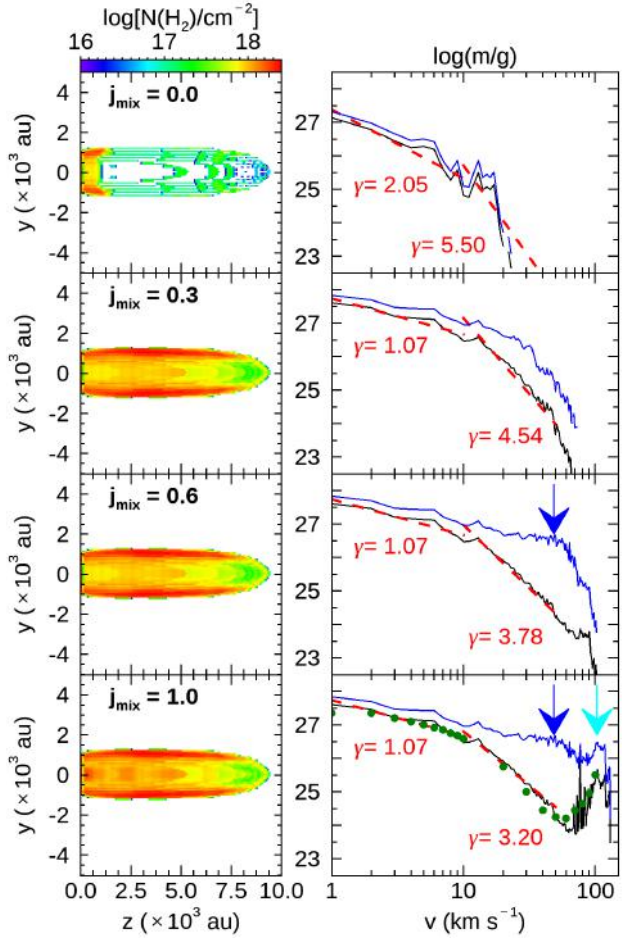

400 yr, i=30°
全質量、分子
矢印: パルスによるbump

- j_{mix}が大きいと高速度成分増加→jet由来の分子ガスの寄与。
- 全質量と分子の差は先頭でのH_2の乖離。

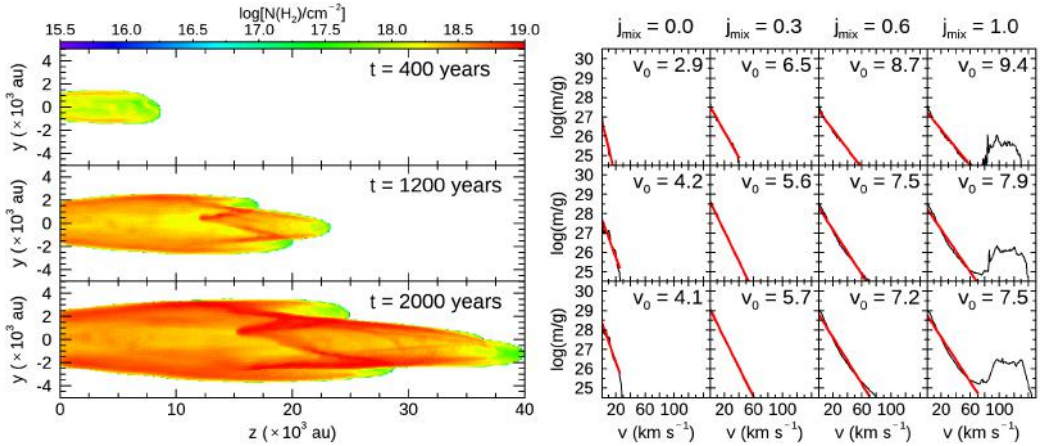

- 大域的にも局所的にもexp(–v/v_0)。
  ← L1157のCO観測でも同じ傾向。
- 他の観測のv0 (1.6-12.5)もage, i, j_{mix}で説明可能。
- 若いほど、説明に必要なj_{mix}（ジェットの寄与）が大きい。

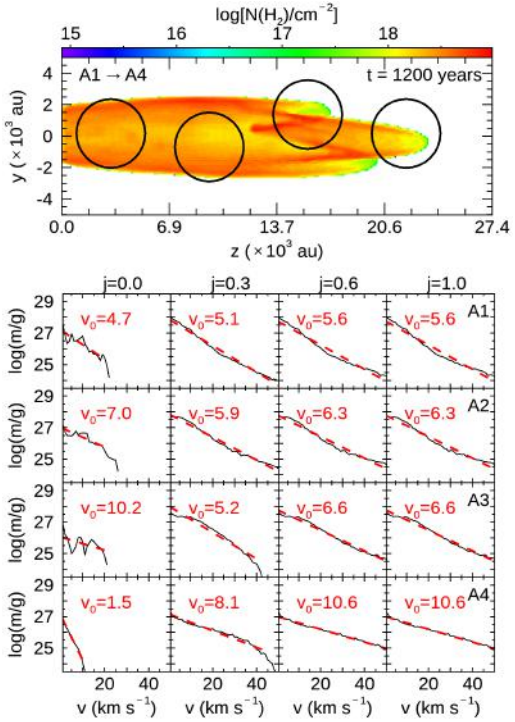

縦が場所に対応。

H_2 mass–velocity relationship from 3D numerical simulations of jet-driven molecular outflows

の続き

A. H. Cerqueira[1], B. Lefloch[2], A. Esquivel[3], P. R. Rivera-Ortiz[2], C. Codella[4,2], C. Ceccarelli[2], and L. Podio[4]

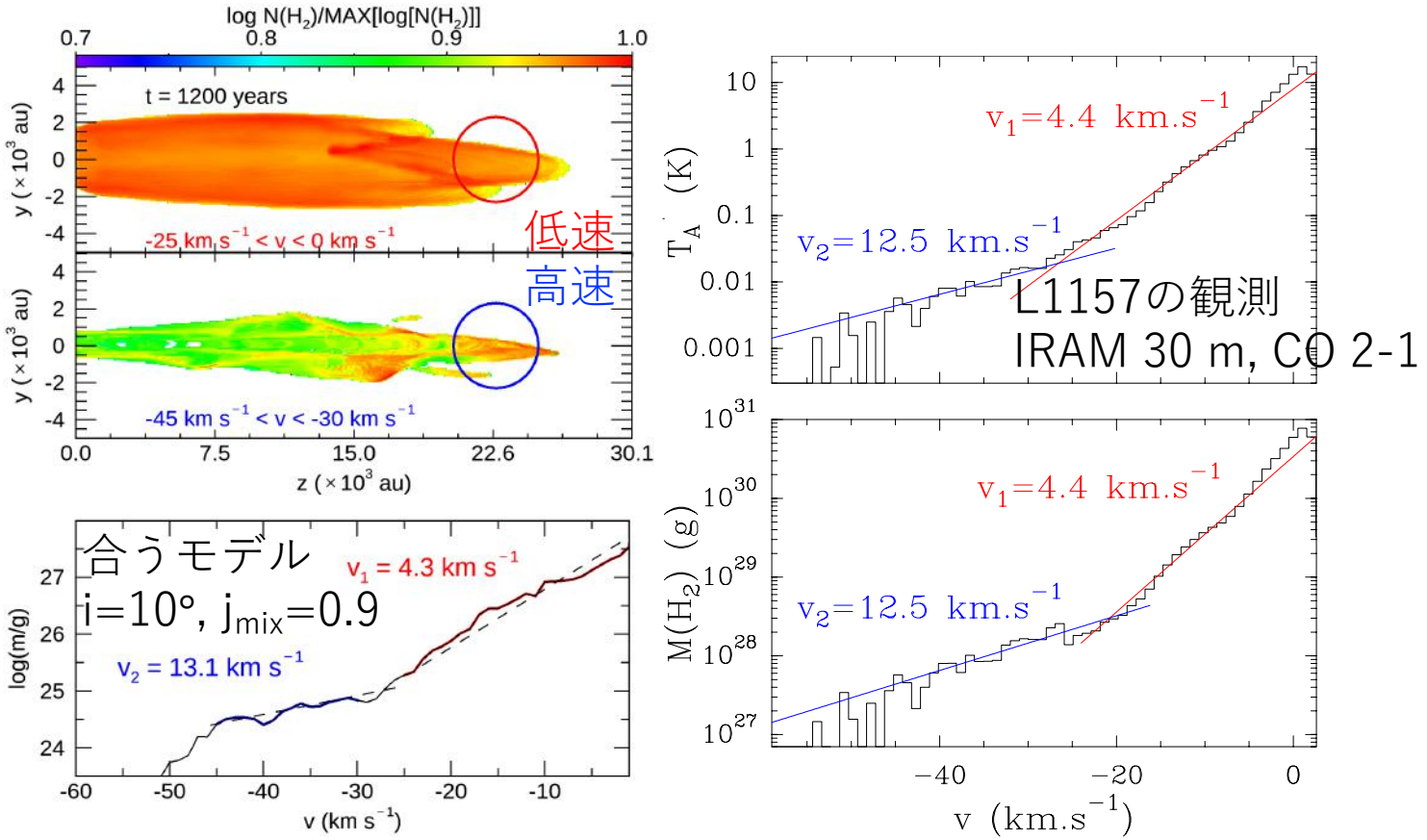

- モデルの高速成分はjet shock impact region (Mach disk)だけではなく、フィラメント状。
- 高速分子流（L1157など）全体を干渉計で観測すればわかる。

The age of the carina young association and potential membership of HD 95086

Mark Booth [1]★ Carlos del Burgo[2,3] and Valeri V. Hambaryan [1,4]

Carina is a nearby young stellar association. So far, only a small number of stars have been clearly identified as members of this association. In this paper, we reanalyse the membership of the association in light of *Gaia* DR2 data, in particular finding that HD 95086 is a potential member (probability of 71 per cent). This star is noteworthy as one of the few stars that hosts both a detected debris disc and a directly imaged planet. It has previously only been considered as a potential member of the Lower Centaurus Crux (LCC) – part of the Scorpius–Centaurus association. We also reanalyse the age of the Carina association. Using a Bayesian inference code applied to infer a solution from stellar evolution models for the most probable (>99 per cent) members of Carina, we infer an age for the association of $13.3^{+1.1}_{-0.6}$ Myr, much younger than previous studies. Whilst we have revised HD 95086's association membership from LCC to Carina, the fact that we also find Carina to have a younger age, similar to that of LCC, means that the estimates of HD 95086b's mass remain unchanged. However, the younger age of Carina does mean that the companion to another Carina member, HD 44627 (AB Pic), has a mass that is more clearly in the planet rather than brown dwarf range.

Carinaの明らかなメンバーは少ない。Gaia DR2で再解析。デブリ円盤と惑星を持つHD95086が71%でメンバー。確実なメンバーと星進化を使ってCarinaの年齢を13 Myrととても若く更新。HD44627の伴星が惑星質量ということになる。

The Explosion in Orion-KL as Seen by Mosaicking the Magnetic Field with ALMA

Paulo C. Cortes[1,2], Valentin J. M. Le Gouellec[3,4], Charles L. H. Hull[2,5,12], Josep M. Girart[6,7], Fabien Louvet[4,8], Edward B. Fomalont[1,2], Seiji Kameno[2,5,9], George A. Moellenbrock[10], Hiroshi Nagai[9,11], Kouichiro Nakanishi[9,11], and Eric Villard[2,3]

We present the first linear-polarization mosaicked observations performed by the Atacama Large Millimeter/submillimeter Array (ALMA). We mapped the Orion-KLeinmann-Low (Orion-KL) nebula using super-sampled mosaics at 3.1 and 1.3 mm as part of the ALMA Extension and Optimization of Capabilities program. We derive the magnetic field morphology in the plane of the sky by assuming that dust grains are aligned with respect to the ambient magnetic field. At the center of the nebula, we find a quasi-radial magnetic field pattern that is aligned with the explosive CO outflow up to a radius of approximately 12″ (∼5000 au), beyond which the pattern smoothly transitions into a quasi-hourglass shape resembling the morphology seen in larger-scale observations by the James-Clerk-Maxwell Telescope (JCMT). We estimate an average magnetic field strength $\langle B \rangle = 9.4$ mG and a total magnetic energy of 2×10^{45} erg, which is three orders of magnitude less than the energy in the explosive CO outflow. We conclude that the field has been overwhelmed by the outflow and that a shock is propagating from the center of the nebula, where the shock front is seen in the magnetic field lines at a distance of ∼5000 au from the explosion center.

ALMA初の偏波モザイク。Orion-KL。磁場が中心の動径方向から外の砂時計へ。
B=9.4 mG、CO分子流よりエネルギーが３桁小さい。

The SEDIGISM survey: molecular clouds in the inner Galaxy

A. Duarte-Cabral[1★], D. Colombo[2★], J. S. Urquhart[3★], A. Ginsburg[4], D. Russeil[5], F. Schuller[2], L. D. Anderson[6], P. J. Barnes[7,8], M. T. Beltrán[9], H. Beuther[10], S. Bontemps[11], L. Bronfman[12], T. Csengeri[11], C. L. Dobbs[13], D. Eden[14], A. Giannetti[2], J. Kauffmann[15], M. Mattern[2], S.-N. X. Medina[2], K. M. Menten[2], M.-Y. Lee[2,16], A. R. Pettitt[17], M. Riener[10], A. J. Rigby[1], A. Traficante[18], V. S. Veena[19], M. Wienen[2], F. Wyrowski[2], C. Agurto[20], F. Azagra[20], R. Cesaroni[9], R. Finger[12], E. Gonzalez[20], T. Henning[10], A. K. Hernandez[21], J. Kainulainen[2,22], S. Leurini[2,23], S. Lopez[4], F. Mac-Auliffe[20], P. Mazumdar[2], S. Molinari[18], F. Motte[24], E. Muller[25], Q. Nguyen-Luong[15], R. Parra[20], J.-P. Perez-Beaupuits[20], F. M. Montenegro-Montes[20], T. J. T. Moore[14], S. E. Ragan[1], A. Sánchez-Monge[19], A. Sanna[2], P. Schilke[19], E. Schisano[18], N. Schneider[19], S. Suri[19], L. Testi[19], K. Torstensson[20], P. Venegas[20], K. Wang[26] and A. Zavagno[5]

We use the ^{13}CO (2–1) emission from the SEDIGISM (Structure, Excitation, and Dynamics of the Inner Galactic InterStellar Medium) high-resolution spectral-line survey of the inner Galaxy, to extract the molecular cloud population with a large dynamic range in spatial scales, using the Spectral Clustering for Interstellar Molecular Emission Segmentation (SCIMES) algorithm. This work compiles a cloud catalogue with a total of 10 663 molecular clouds, 10 300 of which we were able to assign distances and compute physical properties. We study some of the global properties of clouds using a science sample, consisting of 6664 well-resolved sources and for which the distance estimates are reliable. In particular, we compare the scaling relations retrieved from SEDIGISM to those of other surveys, and we explore the properties of clouds with and without high-mass star formation. Our results suggest that there is no single global property of a cloud that determines its ability to form massive stars, although we find combined trends of increasing mass, size, surface density, and velocity dispersion for the sub-sample of clouds with ongoing high-mass star formation. We then isolate the most extreme clouds in the SEDIGISM sample (i.e. clouds in the tails of the distributions) to look at their overall Galactic distribution, in search for hints of environmental effects. We find that, for most properties, the Galactic distribution of the most extreme clouds is only marginally different to that of the global cloud population. The Galactic distribution of the largest clouds, the turbulent clouds and the high-mass star-forming clouds are those that deviate most significantly from the global cloud population. We also find that the least dynamically active clouds (with low velocity dispersion or low virial parameter) are situated further afield, mostly in the least populated areas. However, we suspect that part of these trends may be affected by some observational biases (such as completeness and survey limitations), and thus require further follow up work in order to be confirmed.

銀河系内側の10663個の分子雲。^{13}CO 2-1。大質量星形成と単独で相関する分子雲の性質はない。大きく、乱流が強く、大質量星を形成する分子雲は大局的な分布から外れている。

Temperature Structure of the Pipe Nebula Studied by the Intensity Anomaly of the OH 18 cm Transition

Yuji Ebisawa[1], Nami Sakai[2], Karl M. Menten[3], Yoko Oya[1], and Satoshi Yamamoto[1]

We present observations of the four hyperfine structure components of the OH 18 cm transition (1612, 1665, 1667, and 1720 MHz) toward a filamentary dark cloud, the Pipe nebula, with the Green Bank Telescope. A statistical equilibrium analysis is applied to the spectra, and the kinetic temperature of a diffuse molecular gas surrounding dense cores is determined accurately; the derived temperature ranges from 40 to 75 K. From this result, we assess the heating effect on the filamentary structure of the nebula's "stem" region due to UV photons from a nearby star θ-Ophiuchi and a possible filament–filament collision in the interface of the "stem" and "bowl" regions. In the stem region, the gas kinetic temperature is found to be almost independent of the apparent distance from θ-Ophiuchi: the UV-heating effect by the star is not visible. On the other hand, the gas kinetic temperature is raised, as high as $\sim$75 K, at the interface of the two filamentary structures. This result provides us with additional support for the filament–filament collision scenario in the Pipe nebula.

Green Bank Telescope, OH 18 cm, Pipe nebula。
正確なT_k=40-75 K。幹ではT_kがθ-Ophiuchiからの距離に依らないのでUV-heating無し。
二つのフィラメントの交差点に向かってT_kが増加。フィラメント衝突。

The GRAVITY young stellar object survey

IV. The CO overtone emission in 51 Oph at sub-au scales

GRAVITY Collaboration: M. Koutoulaki[1,2,3,4,⋆], R. Garcia Lopez[1,2,3], A. Natta[2], R. Fedriani[2,3,5], A. Caratti o Garatti[1,2,3], T. P. Ray[2], D. Coffey[2,1], W. Brandner[1], C. Dougados[16], P. J. V. Garcia[7,8,11], L. Klarmann[1], L. Labadie[6], K. Perraut[16], J. Sanchez-Bermudez[1,18], C.-C. Lin[1,19], A. Amorim[8,17], M. Bauböck[9], M. Benisty[16,14], J. P. Berger[16], A. Buron[9], P. Caselli[9], Y. Clénet[10], V. Coudé du Foresto[10], P. T. de Zeeuw[15,9], G. Duvert[16], W. de Wit[11], A. Eckart[6,12], F. Eisenhauer[9], M. Filho[7,8,11], F. Gao[9], E. Gendron[10], R. Genzel[9,13], S. Gillessen[9], R. Grellmann[6], M. Habibi[9], X. Haubois[11], F. Haussmann[9], T. Henning[1], S. Hippler[1], Z. Hubert[16], M. Horrobin[6], A. Jimenez Rosales[9], L. Jocou[16], P. Kervella[10], J. Kolb[11], S. Lacour[10], J.-B. Le Bouquin[16], P. Léna[10], H. Linz[1], T. Ott[9], T. Paumard[10], G. Perrin[10], O. Pfuhl[4], M. C. Ramírez-Tannus[1], C. Rau[9], G. Rousset[10], S. Scheithauer[1], J. Shangguan[9], J. Stadler[9], O. Straub[9], C. Straubmeier[6], E. Sturm[9], E. van Dishoeck[9,15], F. Vincent[10], S. von Fellenberg[9], F. Widmann[9], E. Wieprecht[9], M. Wiest[6], E. Wiezorrek[9], S. Yazici[9,6], and G. Zins[11]

Context. 51 Oph is a Herbig Ae/Be star that exhibits strong near-infrared CO ro-vibrational emission at 2.3 μm, most likely originating in the innermost regions of a circumstellar disc.
Aims. We aim to obtain the physical and geometrical properties of the system by spatially resolving the circumstellar environment of the inner gaseous disc.
Methods. We used the second-generation Very Large Telescope Interferometer instrument GRAVITY to spatially resolve the continuum and the CO overtone emission. We obtained data over 12 baselines with the auxiliary telescopes and derive visibilities, and the differential and closure phases as a function of wavelength. We used a simple local thermal equilibrium ring model of the CO emission to reproduce the spectrum and CO line displacements.
Results. Our interferometric data show that the star is marginally resolved at our spatial resolution, with a radius of $\sim 10.58 \pm 2.65\, R_\odot$. The K-band continuum emission from the disc is inclined by $63° \pm 1°$, with a position angle of $116° \pm 1°$, and 4 ± 0.8 mas (0.5 ± 0.1 au) across. The visibilities increase within the CO line emission, indicating that the CO is emitted within the dust-sublimation radius. By modelling the CO bandhead spectrum, we derive that the CO is emitted from a hot ($T = 1900$–2800 K) and dense ($N_{CO} = (0.9\text{–}9) \times 10^{21}$ cm^{-2}) gas. The analysis of the CO line displacement with respect to the continuum allows us to infer that the CO is emitted from a region 0.10 ± 0.02 au across, well within the dust-sublimation radius. The inclination and position angle of the CO line emitting region is consistent with that of the dusty disc.
Conclusions. Our spatially resolved interferometric observations confirm the CO ro-vibrational emission within the dust-free region of the inner disc. Conventional disc models exclude the presence of CO in the dust-depleted regions of Herbig AeBe stars. Ad hoc models of the innermost disc regions, that can compute the properties of the dust-free inner disc, are therefore required.

VLTI, GRAVITY
CO ro-vibrational
2.3 μm
Herbig disk
連続波で10.6 R_{sun}の星と0.5 auの円盤。
COが0.1 au, 1900-2800 K, 0.9-9x10^{21} cm^{-2}から。
dust-sublimationより内側。